Animal Nutrition 9 (2022) 7–15

Contents lists available at ScienceDirect

Animal Nutrition

journal homepage: http://www.keaipublishing.com/en/journals/aninu/

Original Research Article

Hydroxyproline alleviates 4-hydroxy-2-nonenal-induced DNA damage and apoptosis in porcine intestinal epithelial cells

Yun Ji [a, b], Yu He [a], Ying Yang [a], Zhaolai Dai [a], Zhenlong Wu [a, b, *]

[a] State Key Laboratory of Animal Nutrition, Department of Animal Nutrition and Feed Science, China Agricultural University, Beijing 100193, China
[b] Beijing Advanced Innovation Center for Food Nutrition and Human Health, China Agricultural University, Beijing 100193, China

ARTICLE INFO

Article history:
Received 22 April 2021
Received in revised form
14 July 2021
Accepted 8 August 2021
Available online 16 October 2021

Keywords:
Hydroxyproline
Apoptosis
DNA damage
4-Hydroxy-2-nonenal
Oxidative stress

ABSTRACT

Oxidative stress has been confirmed in relation to intestinal mucosa damage and multiple bowel diseases. Hydroxyproline (Hyp) is an imino acid abundant in sow's milk. Compelling evidence has been gathered showing the potential antioxidative properties of Hyp. However, the role and mechanism of Hyp in porcine intestinal epithelial cells in response to oxidative stress remains unknown. In this study, small intestinal epithelial cell lines of piglets (IPEC-1) were used to evaluate the protective effects of Hyp on 4-hydroxy-2-nonenal (4-HNE)-induced oxidative DNA damage and apoptosis. IPEC-1 pretreated with 0.5 to 5 mmol/L Hyp were exposed to 4-HNE (40 μmol/L) in the presence or absence of Hyp. Thereafter, the cells were subjected to apoptosis detection by Hoechst staining, flow cytometry, and Western blot or DNA damage analysis by comet assay, immunofluorescence, and reverse-transcription quantitative PCR (RT-qPCR). Cell apoptosis and the upregulation of cleaved-caspase-3 induced by 4-HNE (40 μmol/L) were inhibited by 5 mmol/L of Hyp. In addition, 5 mmol/L Hyp attenuated 4-HNE-induced reactive oxygen species (ROS) accumulation, glutathione (GSH) deprivation and DNA damage. The elevation in transcription of *GADD45a* (growth arrest and DNA-damage-inducible protein 45 alpha) and *GADD45b* (growth arrest and DNA-damage-inducible protein 45 beta), as well as the phosphorylation of H2AX (H2A histone family, member X), p38 MAPK (mitogen-activated protein kinase), and JNK (c-Jun N-terminal kinase) in cells treated with 4-HNE were alleviated by 5 mmol/L Hyp. Furthermore, Hyp supplementation increased the protein abundance of Krüppel like factor 4 (KLF4) in cells exposed to 4-HNE. Suppression of KLF4 expression by kenpaulone impeded the resistance of Hyp-treated cells to DNA damage and apoptosis induced by 4-HNE. Collectively, our results indicated that Hyp serves to protect against 4-HNE-induced apoptosis and DNA damage in IPEC-1 cells, which is partially pertinent with the enhanced expression of KLF4. Our data provides an updated explanation for the nutritional values of Hyp-containing animal products.

1. Introduction

The intestinal epithelium is known as a tissue with high self-renewal capacity in mammalians (Umar, 2010). Redox homeostasis is critical for the absorption and metabolism of nutrients in intestinal epithelial cells, as well as the integrity of the intestinal mucosa (Circu and Aw, 2011). Excessive intracellular accumulation of reactive oxygen species (ROS) may lead to lipid peroxidation, producing malondialdehyde (MDA) and 4-hydroxy-2-nonenal (4-HNE) (Ayala et al., 2014). Growing evidence indicates that 4-HNE functions as a vital second messenger of oxidative stress, damaging macromolecules such as DNA, protein, and lipid, and thus amplifying cellular injury in various cell types (Okada et al., 1999; Almeida et al., 2009; Yang et al., 2019). Consistently, 4-HNE-induced oxidative damage has been implicated in a variety of cellular processes, including cell proliferation, differentiation, DNA damage, apoptosis, and the development of intestinal diseases (Circu and Aw, 2012). Therefore, it is of significance to explore the detrimental effect of oxidative stress on DNA integrity and

* Corresponding author.
E-mail address: bio2046@hotmail.com (Z. Wu).
Peer review under responsibility of Chinese Association of Animal Science and Veterinary Medicine.

Production and Hosting by Elsevier on behalf of KeAi

https://doi.org/10.1016/j.aninu.2021.08.003

underlying mechanism, which may assist in the development of the potential strategies for maintaining intestinal homeostasis.

The sows' milk is the main source of nutrients for the growth and development of neonates (Spencer et al., 2003). We previously reported that the concentration of hydroxyproline (Hyp; including both free and peptide-bond form) ranged from 6.3 to 9.0 mmol/L in sow's milk (Wang et al., 2013), which is higher than that of other amino acids. However, the functional role of Hyp in the intestine of neonates is not well-defined. Biochemically, Hyp is known as a key component for the synthesis of collagen in animals (Hausmann and Neuman, 1961). Milic et al. (2015) demonstrated that Hyp has the ability to neutralize hydroxyl radicals (·OH) in vitro, indicating an anti-oxidative capacity to ROS insult. In addition, peptides derived from porcine collagen which is rich in Hyp exhibit potent radical-scavenging ability (Ao and Li, 2012). Moreover, accumulated evidence indicates that Hyp content in cultured cells and human urine samples is increased in response to oxidative stress and hypoxic conditions due to enhanced degradation of collagen (Takahashi et al., 2000; Lee et al., 2011). These findings hint of a potential effect of Hyp in maintaining intracellular redox state. The present study aims to test the hypothesis that Hyp attenuates 4-HNE-induced oxidative DNA damage and apoptosis, and to elucidate the potential mechanisms.

2. Materials and methods

2.1. Reagents and chemicals

Trans-4-hydroxyproline-L-proline was bought from Sigma (St. Louis, MO, USA). 4-HNE was purchased from Cayman Chemical (Ann Arbor, MI, USA). Dulbecco's modified eagle medium (DMEM)-F12 medium and fetal bovine serum (FBS) were from GIBCO-BRL (Grand Island, NY, USA). DMEM medium was custom-made from GIBCO-BRL (Grand Island, NY, USA). Histone H2AX Monoclonal Antibody (pSer139) was bought from Epigentek (Farmingdale, NY, USA). Beta-actin antibody was from Santa Cruz Biotechnology (Santa Cruz, CA, USA). Antibodies for phospho-p38 MAPK (mitogen-activated protein kinase, Thr180/Tyr182), p38 MAPK, phospho- JNK (c-Jun N-terminal kinase, Thr183/Tyr185), JNK, cleaved-caspase-3 were obtained from Cell Signaling Technology (Beverly, MA, USA). Peroxidase-conjugated and Fluorescein (FITC)-conjugated secondary antibodies were from Huaxingbio Biotechnology Co. (Beijing, China). TRIzon Reagent was obtained from Aidlab biotech Co. (Beijing, China). PrimeScript RT Master Mix and SYBR Premix EX Taq II kits were purchased from Takara Biotechnology Co. (Dalian, China).

2.2. Cell culture

Intestinal porcine epithelial cell line-1 (IPEC-1) cells were maintained in DMEM/F-12 (1:1) supplemented with 10% fetal bovine serum (FBS), 1% penicillin–streptomycin and were incubated at 37 °C in a humidified 5% CO_2 atmosphere.

2.3. Cell counting kit-8 (CCK-8) assay

Cell viability was determined by CCK-8 (ZOMANBIO Biotechnology Co., Beijing, China) following the manufacturer's instruction. IPEC-1 cells were seeded in a 96-well plate at a density of 1×10^4 cells/well in 100 μL growth medium. After an overnight incubation, cells were pretreated with indicated doses of Hyp for 12 h in DMEM medium supplemented with 5% FBS after a starvation in serum-free DMEM medium for 6 h and then were subjected to DMEM medium containing 4-HNE or 4-HNE plus Hyp for designated time points. Following the addition of 10 μL CCK-8 reagent to each well, the plate was incubated for 30 min at 37 °C. Subsequently, the absorbance was measured by a microplate reader at 450 nm.

2.4. Hoechst staining

To visualize the apoptotic cells through nuclear change, the nuclei of living cells were stained with Hoechst 33,342. After a 6-h starvation in serum-free DMEM medium, cells pretreated with Hyp for 12 h in DMEM containing 5% FBS were exposed to 4-HNE (40 μmol/L) in DMEM for 6 h. Then, the cells were stained with Hoechst 33,342 (5 μg/mL) for 10 min, followed by photographing using a fluorescence microscope (Zeiss, Germany). The apoptotic cells showed the nuclei with high-density fluorescence.

2.5. Flow cytometric analysis

After treatment, the collected cells were washed with PBS and then resuspended in 1 × binding buffer provided by the manufacturer (Jiamay Biotechnology, Beijing, China). Following 20 min incubation with FITC-Annexin V and 5-min staining with PI at room temperature, the cell pellets were analyzed by flow cytometer (Beckman Coulter, USA). The results were presented by a dot plot of PI-fluorescence (y-axis) versus FITC-fluorescence (x-axis).

2.6. ROS detection

The generation of ROS was determined using 2′-7′dichlorofluorescin diacetate (DCFH-DA, Beyotime Biotechnology Co., Shanghai, China), which can be oxidized to dichlorofluorescein (DCF) with high fluorescence in cells. Cells were starved for 6 h in serum-free DMEM medium and then pretreated with or without Hyp (2 or 5 mmol/L) for 12 h at 37 °C before being stimulated with 4-HNE (40 μmol/L) for 3 h in the presence or absence of Hyp. Subsequently, the cells were exposed to 10 μmol/L DCFH-DA for an additional 30 min at 37 °C and observed under a fluorescence microscope (Zeiss, Germany). DCF fluorescence intensity was quantified using Image J software (NIH, USA).

2.7. Glutathione (GSH) determination

The intracellular content of glutathione was determined using a commercial kit (Beyotime Biotechnology Co., Shanghai, China). Briefly, the harvested cells were mixed with 5% metaphosphoric acid and subjected to repeated freeze-thaw. The samples then were centrifuged to collect the supernatant. The level of total glutathione was detected by DTNB (5, 5′-dithio 2-p-nitrobenzoic acid) method using spectrophotometry at 412 nm. Protein concentration was quantified by bicinchoninic acid (BCA) assay using an equal volume of cell pellets.

2.8. Comet assay

Comet assay (single cell gel electrophoresis) was performed following the protocol described by Speit and Rothfuss (2012) with slightly modification. In brief, the IPEC-1 cells suspended in 0.5% low-melting-point agarose after treatment were added onto glass microscope slides precoated with a layer of 1.5% normal-melting-point agarose. The slides were soaked in lysis solution (2.5 mol/L NaCl, 100 mmol/L EDTA, 10 mmol/L Tris [pH 10.0], 1% Triton X-100 and 10% DMSO) at 4 °C for 2 h and then were subjected to horizontal electrophoresis at 25 V for 20 min. Thereafter, the samples were placed in a neutralization buffer for 10 min. After rinsing, the slides were stained with 10 μg/mL of propidium iodide in distilled

water for 20 min, followed by images being captured with a fluorescence microscope (Zeiss, Germany).

2.9. Immunofluorescence

Cells were fixed in 4% paraformaldehyde for 15 min at room temperature and then washed 3 times with cold PBS. After permeabilization with 0.1% Triton X-100 in PBS for 15 min, they were washed 3 times with PBS and incubated with 1% goat serum for 1 h at room temperature. Cells were incubated with 1% goat serum containing primary antibody of p-H2AX (Ser139) (1:200 dilution) for 16 h at 4 °C, after which they were washed 3 times with PBS for 5 min each. The samples then were followed by an incubation of FITC-conjugate secondary antibody (1:100 dilution) for 1 h at room temperature and 3 times washing with PBS. The images were captured by a fluorescence microscope (Zeiss, Germany).

2.10. RNA extraction and reverse-transcription quantitative PCR (RT-qPCR)

Total RNA was extracted using a TRIzol kit (Aidlab biotech Co., Beijing, China) according to the instructions provided by the manufacturer. The cDNA was obtained by reverse transcription of total RNA, which was carried out by a reverse transcription kit (PrimeScript RT Master Mix). The qPCR was conducted by the SYBR green mix and specific primers for the genes of porcine with a Real time PCR system (ABI 7500) by using a real time PCR kit (SYBR Premix EX Taq II) following the instructions. Beta-actin was used as a reference gene. The primer sequences for each gene were designed as follows: *β-actin*, forward 5′-TCTTCCAGCCCTCCTTCTTG-3′ and reverse 5′-TCCTTCCTGATGTCCACGTC-3’; *GADD45a* (growth arrest and DNA-damage-inducible protein 45 alpha), forward 5′-GCTGGTGACGAATCCACATT-3′ and reverse 5′-TCACTGGAACCCACTGATCC-3’; *GADD45b* (growth arrest and DNA-damage-inducible protein 45 beta), forward 5′-AGTCGTTTTGCTGTGACAACG-3′ and reverse 5′-CATCTGTGTGAGGGTTCGTGA-3’; *GADD45g* (growth arrest and DNA-damage-inducible protein 45 gamma), forward 5′-ACAACGTGACCTTTTGCGTG-3′ and reverse 5′-TTCTCACAGCAGAACGCCTG-3’; *HO-1* (heme oxygenase-1), forward 5′-GGCCAGGTCCTCAAGAAGAT-3′ and reverse 5′-GAAAGTGAAGAAGGCCAGGC-3’. The relative expression levels for target genes were calculated by $2^{-\Delta\Delta CT}$ method (Livak and Schmittgen, 2001).

2.11. Western blot analysis

The cell pellets were dissolved and vortexed in RIPA buffer (10 mmol/L Tris—HCl, pH 7.4; 150 mmol/L NaCl; 10 mmol/L EDTA; 1% NP-40; 0.1% SDS) supplemented with protease and phosphatase inhibitor. After centrifuging, the supernatant of the dissolved pellets was quantified by BCA method. The lysates containing 25 μg protein were subjected to SDS-PAGE (5% stacking gel and 12% separation gel) and then transferred onto a PVDF membrane via transfer buffer by the semi-dry method.

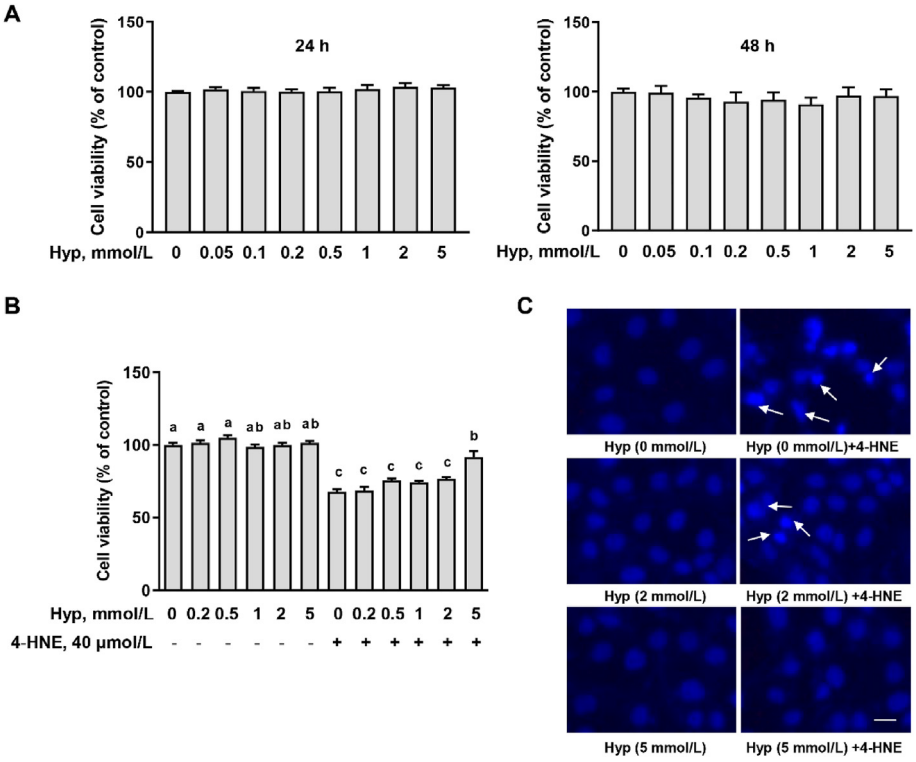

Fig. 1. Hyp attenuated 4-HNE-induced IPEC-1 cell death. (A) Effect of Hyp on the viability of IPEC-1 cells. Following a starvation in serum-free DMEM medium for 6 h, cells were treated with various concentrations of Hyp in DMEM medium (5% serum) for 24 or 48 h. The results were expressed as mean ± SEM. $n = 6$. (B) IPEC-1 cells were exposed to serum starvation in DMEM medium for 6 h and then pretreated with indicated concentrations of Hyp (0.2, 0.5, 1, 2 and 5 mmol/L) in DMEM medium supplemented with 5% FBS for 12 h, followed by 4-HNE exposure in the present or absence of Hyp for 6 h. Cell viability was analyzed by CCK-8 assay. Values are expressed as mean ± SEM. $n = 6$. Different letters express significant differences among groups by Tukey's multiple comparison test, $P < 0.05$. (C) Hoechst staining of IPEC-1 cells. Cells were subjected to 4-HNE (40 μmol/L) with or without Hyp for 6 h after 12 h pre-incubation of Hyp (2 mmol/L or 5 mmol/L), followed by staining with Hoechst 33,342 for 10 min. The scale bar represents 20 μm. Hyp = hydroxyproline; IPEC-1 = intestinal porcine epithelial cell line-1; 4-HNE = 4-hydroxy-2-nonenal; CCK-8 = cell counting kit-8.

The PVDF membrane was incubated in 5% BSA containing primary antibody (dilution of 1:2,000) overnight at 4 °C after blocking in 5% defatted milk for 1 h at room temperature. Following washing 3 times with washing buffer (Tris-buffered saline with Tween 20), the membrane was further incubated with horseradish peroxidase-conjugated secondary antibodies (1:5,000 dilution) for 1 h in 5% skim milk at room temperature and washed 3 times again with washing buffer. Posteriorly, protein bands were visualized with an enhanced chemiluminescence kit using an ImageQuant LAS 4000 mini system (GE Healthcare). The intensity of individual protein bands was quantified by Image J software (NIH, USA).

2.12. Statistical analysis

Statistical analysis was carried out by one-way or two-way ANOVA using SAS 9.0 software (SAS Institute Inc., Cary, NC, USA), followed by Tukey's multiple comparison test. Student's t-test was used for the comparison between 2 groups. Values were expressed as the mean ± standard error of the mean (SEM). $P < 0.05$ was considered to be significant statistically.

3. Results

3.1. Hyp ameliorated 4-HNE-induced cytotoxicity in IPEC-1 cells

Hyp (0.2 to 5 mmol/L) treatment showed no effect on cell viability of IPEC-1 at either 24 or 48 h (Fig. 1A). To determine the effect of Hyp on 4-HNE-induced cytotoxicity, IPEC-1 cells were treated with 40 μmol/L 4-HNE, as previously described (Ji et al., 2016), in the absence or presence of various concentrations of Hyp. As shown, a reduction in cell viability was observed in cells exposed to 4-HNE (40 μmol/L), which was significantly reversed by 5 mmol/L Hyp ($P < 0.05$) (Fig. 1B). Hoechst staining showed that 4-HNE treatment

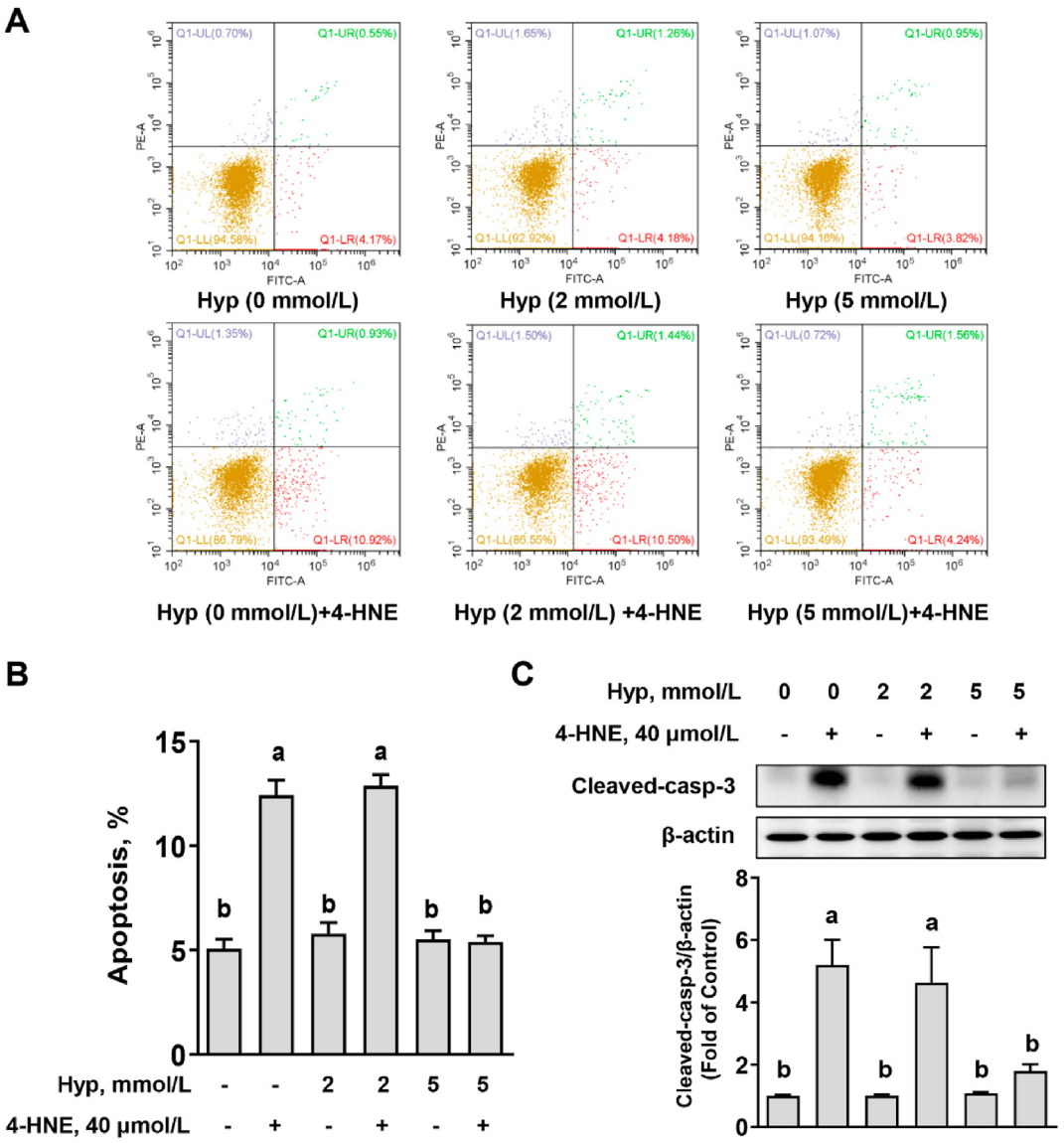

Fig. 2. Hyp protected against 4-HNE-induced apoptosis in IPEC-1 cells. (A) Flow cytometry assay. Cells were pre-incubated in DMEM medium supplemented with 5% FBS and Hyp for 12 h and then exposed to 4-HNE (40 μmol/L) for an additional 6 h before harvested for flow cytometry analysis. (B) Bar chart represents the total percentage of early apoptotic cells plus late apoptotic cells from the analysis results of flow cytometry. (C) Western blot analysis of cleaved-caspase-3 in cells exposed to 4-HNE (40 μmol/L) for 6 h after 12 h pretreatment of various concentrations of Hyp (2 and 5 mmol/L). Data are expressed as mean ± SEM. $n = 3$. Different letters express significant differences among groups by Tukey's multiple comparison test, $P < 0.05$. Hyp = hydroxyproline; 4-HNE = 4-hydroxy-2-nonenal; IPEC-1 = intestinal porcine epithelial cell line-1.

led to the appearance of dense nuclei, a characteristic feature of cell death, which was attenuated by 5 mmol/L Hyp (Fig. 1C). Considering that the protective effect was observed in the presence of 5 mmol/L Hyp, this concentration was used in the subsequent experiments in our study to explore potential mechanisms.

3.2. Hyp reduced 4-HNE-induced apoptosis and caspase-3 activation in IPEC-1 cells

As compared with the control, flow cytometry analysis indicated that 4-HNE treatment resulted in an increase in cell apoptosis as evidenced by the elevated percentage of cells in the early plus late stage of apoptotic process ($P < 0.05$). The addition of 5 mmol/L Hyp attenuated apoptotic cell death induced by 4-HNE ($P < 0.05$) (Fig. 2A, B). Activation of caspase-3 is critical for the progression of apoptotic signaling cascade, therefore, we next determined the protein abundance of cleaved-caspase-3 by Western blot. The upregulation of cleaved-caspase-3 caused by 4-HNE exposure was significantly inhibited by 5 mmol/L of Hyp treatment (Fig. 2C). These data presented here indicated a protective effect of Hyp against 4-HNE-induced cell death in IPEC-1 cells.

3.3. Effect of Hyp on 4-HNE-triggered production of ROS and deprivation of GSH

Generation of ROS by 4-HNE has been implicated in the cellular damage in various types of cells. We next determined the effects of Hyp on 4-HNE-induced ROS accumulation in our cell line model. Cells treated with 4-HNE in the absence or presence of Hyp were labeled with DCFH-DA probe (10 μmol/L) before being subjected to fluorescence microscope observation. As shown, 4-HNE exposure for 3 h led to an elevation of ROS levels in IPEC-1 cells, which was alleviated by 5 mmol/L Hyp ($P < 0.05$) (Fig. 3A, B). In addition, cells treated with 4-HNE exhibited a dramatic reduction in GSH content, which was ameliorated by Hyp ($P < 0.05$) (Fig. 3C).

3.4. Hyp attenuated 4-HNE-induced DNA damage

We next evaluated 4-HNE-induced DNA damage in IPEC-1 cells. As shown, 4-HNE led to enhanced DNA damage as shown by an increase in the intensity of the comet tail (Fig. 4A) and γ-H2AX foci (Fig. 4B). Intriguingly, Hyp treatment ameliorated 4-HNE-induced DNA damage (Fig. 4A) and the formation of γ-H2AX foci (Fig. 4B), indicating a resistance of Hyp to DNA damage. Next, the mRNA levels of genes related to the induction of DNA damage, including *GADD45a*, *GADD45b*, and *GADD45g*, were evaluated by RT-qPCR. We found that 4-HNE-induced upregulation of *GADD45a* and *GADD45b*, instead of *GADD45g*, was suppressed by Hyp (Fig. 4D). In addition, we detected the expression level of *HO-1* which encodes the anti-oxidative enzyme heme oxygenase-1 modulating DNA repair, and observed that 4-HNE-induced an increase in *HO-1*, which was further markedly enhanced in the presence of Hyp (Fig. 4C).

3.5. Hyp reversed 4-HNE-induced phosphorylation of p38 MAPK and JNK

As GADD45 has been implicated in the activation of p38 MAPK and JNK, we determined whether Hyp reduces 4-HNE-induced initiation of p38 MAPK and JNK signaling. As shown in Fig. 4E, F, 4-HNE exposure significantly increased the phosphorylation levels of

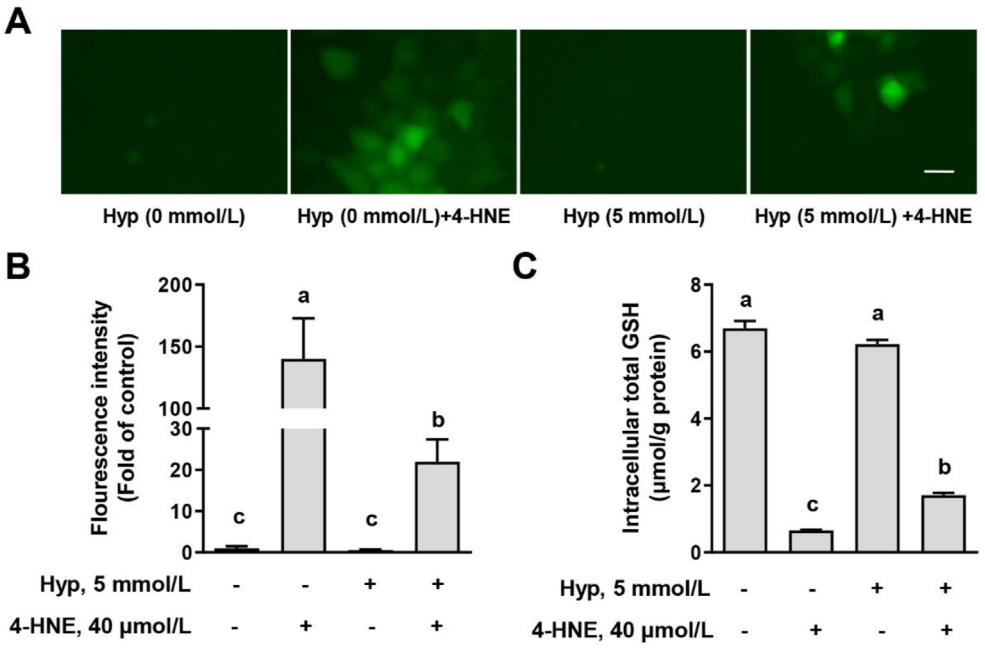

Fig. 3. Hyp mitigated 4-HNE-induced reactive oxygen species (ROS) production and glutathione (GSH) deprivation. (A) Cells were pre-incubated with 5 mmol/L of Hyp for 12 h, followed by an additional treatment with 40 μmol/L 4-HNE for 3 h and then subjected to ROS determination as the procedure described in materials and methods. The scale bar indicates 20 μm. (B) The fluorescence intensity of dichlorofluorescein (DCF) was quantified from 6 images per group by using Image J software. (C) Intracellular GSH content. Cells pretreated with Hyp for 12 h were exposed to 4-HNE for 6 h. Data are shown as mean ± SEM. $n = 3$. Different letters express significant differences among groups by Tukey's multiple comparison test, $P < 0.05$. Hyp = hydroxyproline; 4-HNE = 4-hydroxy-2-nonenal.

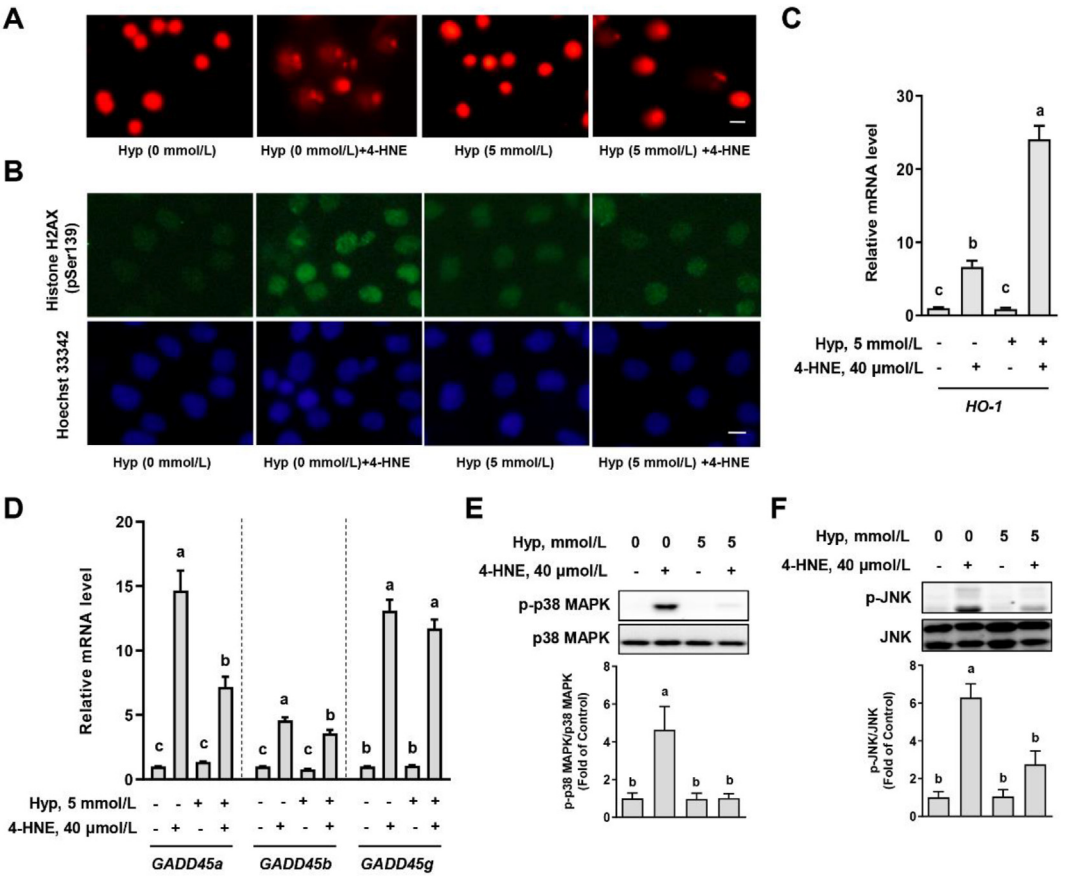

Fig. 4. 4-HNE-triggered DNA damage, *GADD45* expression, and phosphorylation of p38 MAPK and JNK were attenuated while *HO-1* expression was enhanced by Hyp in IPEC-1 cells. Cells were treated with 40 μmol/L 4-HNE for 3 h after pretreated with Hyp for 12 h and then the samples were analyzed by (A) comet assay (scale bar = 20 μm), (B) immunofluorescence (scale bar = 20 μm), (C and D) real-time PCR, or (E and F) Western blot as the protocol mentioned in materials and methods. Beta-actin was taken as a reference for real-time PCR assay. Data are shown as mean ± SEM (n = 3). Different letters express significant differences among groups by Tukey's multiple comparison test, $P < 0.05$. Hyp = hydroxyproline; 4-HNE = 4-hydroxy-2-nonenal; *HO-1* = heme oxygenase-1; *GADD45* = growth arrest and DNA-damage-inducible protein 45; p38 MAPK = p38 mitogen-activated protein kinase; JNK = c-Jun N-terminal kinase.

p38 MAPK and JNK in IPEC-1 cells, which was abolished ($P < 0.05$) by 5 mmol/L of Hyp.

3.6. Krüppel-like factor 4 (KLF4) is involved in the protective effect of Hyp on 4-HNE-induced apoptosis and DNA damage

In order to confirm whether the transcription factor KLF4 is implicated in the protective effect of Hyp against 4-HNE-induced oxidative damage, the expression of KLF4 was detected by Western blot. As shown in Fig. 5A, Hyp increased the abundance of KLF4 induced by a 6-h treatment of 4-HNE in IPEC-1 cells ($P < 0.05$). Treatment with kenpaulone (5 μmol/L), an inhibitor proven to hinder the expression of KLF4, for 12 h resulted in a significant decrease in KLF4 level ($P < 0.05$) (Fig. 5B). Kenpaulone pretreatment significantly enhanced 4-HNE-induced apoptosis and impeded the protective effect of Hyp on 4-HNE-induced apoptosis ($P < 0.05$) (Fig. 5C, D). In addition, the results from comet assay (Fig. 6A) and immunofluorescence (Fig. 6B) of γ-H2AX focus showed that a suppression of KLF4 expression with kenpaulone significantly aggravated 4-HNE-induced DNA damage in IPEC-1 cells and blocked the protective effect of Hyp on DNA damage. This evidence suggests that KLF4 is involved in the alleviation of 4-HNE-induced apoptosis and DNA damage by Hyp.

4. Discussion

Growing evidence suggests that oxidative stress is relevant to the development of intestinal diseases and disruption of barrier function (Bhattacharyya et al., 2014; Wang et al., 2015). Biological macromolecules, including DNA, protein, and lipid, are susceptible to ROS attack due to their biochemical and structural properties (Schieber and Chandel, 2014). Recent studies show that 4-HNE, an end product of peroxidation of n-6 polyunsaturated fatty acid, is cytotoxic to epithelial cells and might be a critical mediator that contributes to DNA damage and cellular dysfunction (Sharma et al., 2008; Chen et al., 2015; Ji et al., 2016). In the present study, IPEC-1, a cell line well used for the evaluation of intestinal barrier function and nutrient metabolism (Wang et al., 2014; Sun et al., 2017), was incubated with 4-HNE in the presence or absence of Hyp, a component of collagen (Wu et al., 2011, Wu et al., 2017). In agreement with previous studies (Choudhury et al., 2004; Yadav et al., 2008), we found that 4-HNE treatment led to increased DNA damage, as shown by an increased intensity of the comet tail and γ-H2AX foci. Activation of histone H2AX at the DNA break site leads to recruitment of proteins implicated in DNA repair (Kinner et al., 2008; Kuo and Yang, 2008). Therefore, H2AX phosphorylation has been widely accepted as a marker for DNA double-strand breaks. In

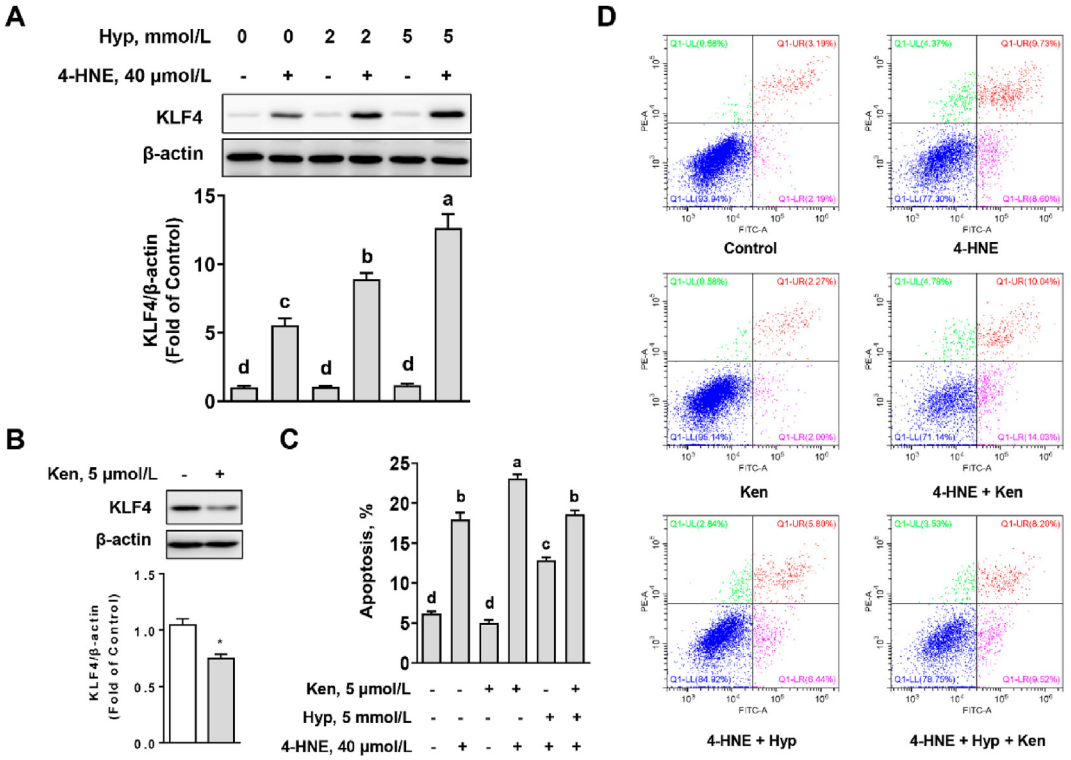

Fig. 5. KLF4 is involved in the protective effect of Hyp on 4-HNE-induced apoptosis in IPEC-1 cells. (A) Cells were pretreated with Hyp (5 mmol/L) for 12 h, followed by co-treated with 40 μmol/L 4-HNE for an additional 6 h before Western blot analysis. Beta-actin was used as internal reference. (B) Cells were treated with kenpaulone (5 μmol/L) for 12 h and then subjected to Western blot analysis. Beta-actin was used as internal reference. (C and D) Flow cytometry analysis of cell apoptosis. The total percentage of early apoptotic cells plus late apoptotic cells was shown in the histogram. Data were expressed as mean ± SEM ($n = 3$). Tukey's method was used for multiple comparison. Different letters indicate significant, $P < 0.05$. KLF4 = Krüppel-like factor 4; Hyp = hydroxyproline; 4-HNE = 4-hydroxy-2-nonenal; IPEC-1 = intestinal porcine epithelial cell line-1; Ken = kenpaulone.

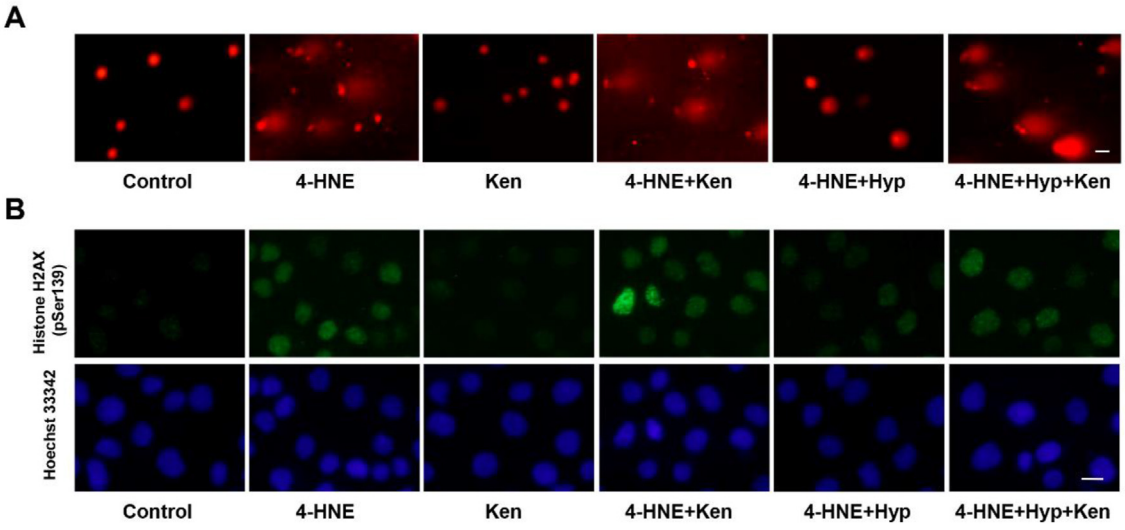

Fig. 6. Inhibition of Krüppel-like factor 4 (KLF4) expression blocked the protective effect of Hyp on 4-HNE-induced DNA damage in IPEC-1 cells. The cells were precultured in DMEM medium containing Hyp with or without 5 μmol/L kenpaulone for 12 h, after which they were incubated in Hyp-containing medium in the presence or absence of 40 μmol/L 4-HNE for 3 h before (A) comet assay or (B) immunofluorescence analysis. The scale bar indicates 20 μm. Hyp = hydroxyproline; 4-HNE = 4-hydroxy-2-nonenal; Ken = kenpaulone.

the present study, the intensity of the comet tail and γ-H2AX foci observed in 4-HNE-treated cells was inhibited by Hyp, indicating a reduced DNA damage in intestinal epithelial cells. This effect of Hyp is mediated, at least partially, by the following mechanisms. First, Hyp is known to limit the generation of hydroxyl radical through the Fenton reaction (Milic et al., 2015), thereby contributing to the mitigation in DNA damage as observed. Second, Hyp is a precursor for the synthesis of glycine (Wu et al., 2011, Wu et al., 2017; Li and Wu, 2018), a substrate for the synthesis of GSH. GSH serves as an intracellular molecule with radical scavenging activity (Rice-Evans et al., 1996), and thus restores the redox homeostasis in coping with free radicals.

GADD45-encoded growth arrest and DNA damage inducing proteins are known as key mediators in response to DNA damage (Zhan, 2005). It has been observed that there was an elevation in the expression of GADD45 during cell apoptosis induced by a variety of agents (Sheikh et al., 2000). In our study, the induction of *GADD45a* and *GADD45b* of cells exposed to 4-HNE was mitigated by Hyp, suggesting a regulatory effect of Hyp on GADD45-mediated cell death. Activated GADD45 induces activation of JNK and p38 MAPK signaling, 2 stress proteins implicated in apoptosis, and thus plays an important part in stress-related cell death (Sheikh et al., 2000; Son et al., 2011). Phosphorylation of p38 MAPK and JNK induced by oxidative stress has been observed in various cell lines (Ravindran et al., 2011; Guo et al., 2012; Park, 2012). Our results showed that 4-HNE significantly increased the phosphorylation levels of JNK and p38 MAPK in IPEC-1 cells, which is consistent with previous observations (Wang et al., 2014). Hyp treatment inhibited the phosphorylation of JNK and p38 MAPK induced by 4-HNE, suggesting that the reduction in DNA damage by Hyp may be related to the inhibition of JNK and p38 MAPK activation. A large body of evidence has shown that the induction of HO-1, an enzyme involved in detoxification and antioxidant process, protects cells against DNA damage and provides an elevated activity of DNA repair (Speit et al., 2000; Mazza et al., 2003; Otterbein et al., 2011). We determined the mRNA levels of HO-1, and observed that 4-HNE-induced induction of HO-1, was enhanced by approximately 3.6-time folds following Hyp treatment. Considering that there was a moderate induction of HO-1 by 4-HNE, the data provided here indicates a threshold of transcriptional level of HO-1 on cellular protection in response to ROS.

KLF4, one of the transcription factors of Krüppel like factor family, is expressed in multiple tissues and participates in various cellular processes such as apoptosis, DNA damage, and cell cycle (McConnell and Yang, 2010). KLF4 serves as a key regulator in the maintenance of homeostasis in the intestinal epithelium (Ghaleb and Yang, 2017). Overexpression of KLF4 significantly reduces DNA damage and apoptosis in colon cells induced by gamma radiation (Ghaleb et al., 2007). Drug-induced DNA damage regulated by KLF4 is closely related to the degree of DNA damage (Zhou et al., 2009). Under sublethal DNA damage, KLF4 induces cell cycle arrest whereas, in response to lethal DNA damage, KLF4 exerts an anti-apoptotic effect (Zhou et al., 2009; Su et al., 2014). Our study corroborated that the mechanism of Hyp in promoting the survival of IPEC-1 cells subjected to 4-HNE-induced lethal oxidative stress is linked to the upregulation of KLF4 expression. Previous studies have shown that knockdown of KLF4 expression aggravates doxorubicin-induced apoptosis (Zhou et al., 2009). In accordance with this study, our results revealed that an inhibition of KLF4 not only exacerbated 4-HNE-induced apoptosis and DNA damage in IPEC-1 cells, but also blocked the protective effect of Hyp on 4-HNE-induced DNA damage and apoptosis.

In conclusion, we provided data showing that lipid peroxidation product 4-HNE exposure led to ROS accumulation, DNA damage, and apoptosis in porcine enterocytes, which was markedly alleviated by Hyp. This favorable effect of Hyp is associated with the suppression of the expression of GADD45-mediated induction of stress protein, p38 MAPK and JNK and upregulation of HO-1. Importantly, the enhanced expression of KLF4 is involved in the protective effect of Hyp against 4-HNE-induced DNA damage and apoptosis in IPEC-1 cells. Supporting the growth and development of piglets, sow's milk is rich in Hyp. Our data support the concept that Hyp is a potential antioxidant in maintaining intestinal mucosal homeostasis.

Author contributions

Yun Ji: Formal analysis, Investigation, Writing – original draft, Writing – review & editing. **Yu He**: Investigation. **Ying Yang**: Formal analysis. **Zhaolai Dai**: Formal analysis. **Zhenlong Wu**: Conceptualization, Writing – review & editing, Supervision.

Declaration of competing interest

We declare that we have no financial and personal relationships with other people or organizations that can inappropriately influence our work, there is no professional or other personal interest of any nature or kind in any product, service and/or company that could be construed as influencing the content of this paper.

Acknowledgments

This work was supported by the National Natural Science Foundation of China (No. 31625025, 31301979), the Zhengzhou 1125 Talent Program, and the Jinxinnong Animal Science Development Foundation.

References

Almeida M, Ambrogini E, Han L, Manolagas SC, Jilka RL. Increased lipid oxidation causes oxidative stress, increased peroxisome proliferator-activated receptor-gamma expression, and diminished pro-osteogenic Wnt signaling in the skeleton. J Biol Chem 2009;284(40):27438–48.
Ao J, Li B. Amino acid composition and antioxidant activities of hydrolysates and peptide fractions from porcine collagen. Food Sci Technol Int 2012;18(5):425–34.
Ayala A, Munoz MF, Arguelles S. Lipid peroxidation: production, metabolism, and signaling mechanisms of malondialdehyde and 4-hydroxy-2-nonenal. Oxid Med Cell Longev 2014;2014:360438.
Bhattacharyya A, Chattopadhyay R, Mitra S, Crowe SE. Oxidative stress: an essential factor in the pathogenesis of gastrointestinal mucosal diseases. Physiol Rev 2014;94(2):329–54.
Chen L, Zong R, Zhou J, Ge L, Zhou T, Ma JX, Liu Z, Zhou Y. The oxidant role of 4-hydroxynonenal in corneal epithelium. Sci Rep 2015;5:10630.
Choudhury S, Pan J, Amin S, Chung FL, Roy R. Repair kinetics of trans-4-hydroxynonenal-induced cyclic 1,N2-propanodeoxyguanine DNA adducts by human cell nuclear extracts. Biochemistry 2004;43(23):7514–21.
Circu ML, Aw TY. Redox biology of the intestine. Free Radic Res 2011;45(11–12):1245–66.
Circu ML, Aw TY. Intestinal redox biology and oxidative stress. Semin Cell Dev Biol 2012;23(7):729–37.
Ghaleb AM, Katz JP, Kaestner KH, Du JX, Yang VW. Kruppel-like factor 4 exhibits antiapoptotic activity following gamma-radiation-induced DNA damage. Oncogene 2007;26(16):2365–73.
Ghaleb AM, Yang VW. Kruppel-like factor 4 (KLF4): what we currently know. Gene 2017;611:27–37.
Guo C, Yuan H, He Z. Melamine causes apoptosis of rat kidney epithelial cell line (NRK-52e cells) via excessive intracellular ROS (reactive oxygen species) and the activation of p38 MAPK pathway. Cell Biol Int 2012;36(4):383–9.
Hausmann E, Neuman WF. Conversion of proline to hydroxyproline and its incorporation into collagen. J Biol Chem 1961;236:149–52.
Ji Y, Dai Z, Wu G, Wu Z. 4-Hydroxy-2-nonenal induces apoptosis by activating ERK1/2 signaling and depleting intracellular glutathione in intestinal epithelial cells. Sci Rep 2016;6:32929.
Kinner A, Wu W, Staudt C, Iliakis G. Gamma-H2AX in recognition and signaling of DNA double-strand breaks in the context of chromatin. Nucleic Acids Res 2008;36(17):5678–94.
Kuo LJ, Yang LX. Gamma-H2AX - a novel biomarker for DNA double-strand breaks. In Vivo 2008;22(3):305–9.
Lee KW, Kim SJ, Park JB, Lee KJ. Relationship between depression anxiety stress scale (DASS) and urinary hydroxyproline and proline concentrations in hospital workers. J Prev Med Public Health 2011;44(1):9–13.
Li P, Wu G. Roles of dietary glycine, proline, and hydroxyproline in collagen synthesis and animal growth. Amino Acids 2018;50(1):29–38.
Livak KJ, Schmittgen TD. Analysis of relative gene expression data using real-time quantitative PCR and the 2(T)(-Delta Delta C) method. Methods 2001;25(4):402–8.

Mazza F, Goodman A, Lombardo G, Vanella A, Abraham NG. Heme oxygenase-1 gene expression attenuates angiotensin II-mediated DNA damage in endothelial cells. Exp Biol Med 2003;228(5):576–83.
McConnell BB, Yang VW. Mammalian Kruppel-like factors in health and diseases. Physiol Rev 2010;90(4):1337–81.
Milic S, Bogdanovic Pristov J, Mutavdzic D, Savic A, Spasic M, Spasojevic I. The relationship of physicochemical properties to the antioxidative activity of free amino acids in Fenton system. Environ Sci Technol 2015;49(7):4245–54.
Okada K, Wangpoengtrakul C, Osawa T, Toyokuni S, Tanaka K, Uchida K. 4-Hydroxy-2-nonenal-mediated impairment of intracellular proteolysis during oxidative stress. Identification of proteasomes as target molecules. J Biol Chem 1999;274(34):23787–93.
Otterbein LE, Hedblom A, Harris C, Csizmadia E, Gallo D, Wegiel B. Heme oxygenase-1 and carbon monoxide modulate DNA repair through ataxia-telangiectasia mutated (ATM) protein. Proc Natl Acad Sci U S A 2011;108(35):14491–6.
Park WH. MAPK inhibitors and siRNAs differentially affect cell death and ROS levels in arsenic trioxide-treated human pulmonary fibroblast cells. Oncol Rep 2012;27(5):1611–8.
Ravindran J, Gupta N, Agrawal M, Bala Bhaskar AS, Lakshmana Rao PV. Modulation of ROS/MAPK signaling pathways by okadaic acid leads to cell death via, mitochondrial mediated caspase-dependent mechanism. Apoptosis 2011;16(2):145–61.
Rice-Evans CA, Miller NJ, Paganga G. Structure-antioxidant activity relationships of flavonoids and phenolic acids. Free Radic Biol Med 1996;20(7):933–56.
Schieber M, Chandel NS. ROS function in redox signaling and oxidative stress. Curr Biol 2014;24(10):R453–62.
Sharma A, Sharma R, Chaudhary P, Vatsyayan R, Pearce V, Jeyabal PV, Zimniak P, Awasthi S, Awasthi YC. 4-Hydroxynonenal induces p53-mediated apoptosis in retinal pigment epithelial cells. Arch Biochem Biophys 2008;480(2):85–94.
Sheikh MS, Hollander MC, Fornance Jr AJ. Role of Gadd45 in apoptosis. Biochem Pharmacol 2000;59(1):43–5.
Son Y, Cheong YK, Kim NH, Chung HT, Kang DG, Pae HO. Mitogen-activated protein kinases and reactive oxygen species: how can ROS activate MAPK pathways? J Signal Transduct 2011;2011:792639.
Speit G, Dennog C, Eichhorn U, Rothfuss A, Kaina B. Induction of heme oxygenase-1 and adaptive protection against the induction of DNA damage after hyperbaric oxygen treatment. Carcinogenesis 2000;21(10):1795–9.
Speit G, Rothfuss A. The comet assay: a sensitive genotoxicity test for the detection of DNA damage and repair. Methods Mol Biol 2012;920:79–90.
Spencer JD, Boyd RD, Cabrera R, Allee GL. Early weaning to reduce tissue mobilization in lactating sows and milk supplementation to enhance pig weaning weight during extreme heat stress. J Anim Sci 2003;81(8):2041–52.
Su C, Sun F, Cunningham RL, Rybalchenko N, Singh M. ERK5/KLF4 signaling as a common mediator of the neuroprotective effects of both nerve growth factor and hydrogen peroxide preconditioning. Age 2014;36(4):9685.
Sun K, Lei Y, Wang R, Wu Z, Wu G. Cinnamicaldehyde regulates the expression of tight junction proteins and amino acid transporters in intestinal porcine epithelial cells. J Anim Sci Biotechnol 2017;8:66.
Takahashi Y, Takahashi S, Shiga Y, Yoshimi T, Miura T. Hypoxic induction of prolyl 4-hydroxylase alpha (I) in cultured cells. J Biol Chem 2000;275(19):14139–46.
Umar S. Intestinal stem cells. Curr Gastroenterol Rep 2010;12(5):340–8.
Wang L, Hou Y, Yi D, Ding B, Zhao D, Wang Z, Zhu H, Liu Y, Gong J, Assaad H, Wu G. Beneficial roles of dietary oleum cinnamomi in alleviating intestinal injury. Front Biosci (Landmark Ed) 2015;20:814–28.
Wang W, Wu Z, Lin G, Hu S, Wang B, Dai Z, Wu G. Glycine stimulates protein synthesis and inhibits oxidative stress in pig small intestinal epithelial cells. J Nutr 2014;144(10):1540–8.
Wang WW, Rezaei R, Wu ZL, Dai ZL, Wang JJ, Wu GY. Concentrations of free and peptide-bound hydroxyproline in the sow's milk and piglet plasma. Amino Acids 2013;45(3). 595-595.
Wu G, Bazer FW, Burghardt RC, Johnson GA, Kim SW, Knabe DA, Li P, Li X, McKnight JR, Satterfield MC, Spencer TE. Proline and hydroxyproline metabolism: implications for animal and human nutrition. Amino Acids 2011;40(4):1053–63.
Wu Z, Hou Y, Dai Z, Hu CA, Wu G. Metabolism, nutrition, and redox signaling of hydroxyproline. Antioxid Redox Signal; 2017.
Yadav UC, Ramana KV, Awasthi YC, Srivastava SK. Glutathione level regulates HNE-induced genotoxicity in human erythroleukemia cells. Toxicol Appl Pharmacol 2008;227(2):257–64.
Yang LL, Chen H, Wang J, Xia T, Sun H, Yuan CH, Liu SL, Chen JB. 4-HNE induces apoptosis of human retinal pigment epithelial cells by modifying HSP70. Curr Med Sci 2019;39(3):442–8.
Zhan Q. Gadd45a, a p53- and BRCA1-regulated stress protein, in cellular response to DNA damage. Mutat Res 2005;569(1–2):133–43.
Zhou Q, Hong Y, Zhan Q, Shen Y, Liu Z. Role for Kruppel-like factor 4 in determining the outcome of p53 response to DNA damage. Cancer Res 2009;69(21):8284–92.